Journal of Sound and Vibration (1999) **227**(3), 647–666
Article No. jsvi.1999.2383, available online at http://www.idealibrary.com on IDEAL®

ACTIVE CONTROL OF MULTI-TONAL NOISE WITH REFERENCE GENERATOR BASED ON ON-LINE FREQUENCY ESTIMATION

S. KIM, Y. PARK

Center for Noise and Vibration Control, Department of Mechanical Engineering, Korea Advanced Institute of Science and Technology, Science Town, Taejeon 305-701, *South Korea*

(*Received* 7 *July* 1998, *and in final form* 8 *May* 1999)

In this paper, a novel active noise control (ANC) structure with a frequency estimator is proposed for systems with multi-tonal noise. The conventional feedforward ANC algorithms need a measured reference signal to calculate the gradient of the squared error and filter coefficients. For ANC systems applied to aircraft or passenger ships, which reference signals are usually measured are so far from seats where engines from the main part of controllers is placed that the scheme might be difficult to implement or very costly. Feedback ANC algorithms which do not require a measure of reference signals, use error signals alone to update the filter and are usually sensitive to measurement noise and unexpected transient noise such as a sneeze, clapping of hands and so on.

The proposed algorithm, which estimates frequencies of the multi-tonal noise in real time using adaptive notch filter (ANF), improves convergence rate, threshold SNR and computational efficiency compared with the conventional ones. The reference signal needed for the feedforward control is not measured directly, but is generated with the estimated frequencies. It has a strong similarity to the conventional IMC-based feedback control because the reference is generated from the error signal in both cases. The proposed ANC algorithm is compared with the conventional IMC-based feedback control algorithm.

Cascade ANF, which has a low computational burden, is used to implement the ANC system in real time. Experiments for verifying efficacy of the proposed algorithm are carried out in the laboratory.

1. INTRODUCTION

For active control of sound and vibration, two types of control strategy have been widely applied. The first one is a feedforward control method, which requires both a reference signal and an error signal, and can attenuate broadband noise as well as narrowband noise. The measured reference signal, which is correlated with the impending primary noise, is used to derive the control input. If the correlation between the reference and the error signal is perfect, it is theoretically possible to make the error signal zero, which can be a very attractive feature. However, if the correlation is only partial, the system only cancels the primary noise components

0022-460X/99/430647 + 20 $30.00/0

that are correlated with the reference signal. Because of its high stability and performance robustness, it has been used in many applications [1]. The second one is a feedback control method, which requires the error signal alone to attenuate periodic noise. Systems with difficulty in obtaining suitable references or active control systems characterized by a narrowband disturbance, typically use feedback control in order to avoid the problems associated with obtaining a reference signal for use in a feedforward LMS configuration. It is well known that a certain level of noise reduction can only be achieved over a limited bandwidth and the smaller the error signal is driven, the higher the control gain must be, and the less stable will be the systems [2].

Active control of harmonic noise has received a great deal of attention because rotating or reciprocating machinery such as engines or fans induce the harmonic noise. As mentioned above, we can obtain good performance for the harmonic noise using a feedforward control method only when a reference is available. For ANC applied to passenger ships or aircraft, engines from which reference signals are usually measured, are so far from seats where the main part of controllers is placed that the scheme might be difficult to implement or costly. Among various feedback methods that do not require reference signals, the internal model control (IMC) technique [3] that alters its feedback structure into a feedforward one has superior performance over other feedback methods for harmonic noise. However, the scheme is sensitive to measurement noise and unexpected transient disturbance (impulse noise) such as a sneeze, clapping hands and so on. Moreover, error signals may increase suddenly due to an impulse noise with a large level of power, which can make the adaptive algorithm unstable. An analogue device, which cancels repetitive vibrations, has been developed [14]. The apparatus exploits the IMC technique to synthesize the reference signal. The synthesized signal is processed by the phase-locked loop to generate the narrowband signal.

In this paper, a new indirect feedback ANC algorithm is proposed for multi-tonal noise. Firstly, we estimate noise signals in the controlled field, using the IMC technique, from the error signals and then estimate its frequencies in real-time. Secondly, we generate sinusoidal signals with the estimated frequencies and use them as reference signals in the conventional feedforward ANC algorithm. If the noise frequencies are exactly estimated, the scheme will be identical to the conventional normalized feedforward method that measures multi-tones directly, except that the smaller order of the adaptive controller may be used because the reference signal of the proposed method has no measurement noise.

We propose a new frequency estimation algorithm with the improved convergence rate, threshold signal-to-noise ratio (SNR) and computational efficiency based on the adaptive notch filter (ANF) with constrained poles and zeros in section 2. Computational efficiency and fast convergence rate is important, because not only should frequency estimation be accurate, but it should also be executed in real time. Among the various methods of frequency estimation, it is well known that the ANF-based method has good tracking capability, low computational complexity and high accuracy [4]. The simulation results show the effectiveness of the proposed algorithm. The proposed ANC algorithm has a strong similarity to the conventional IMC-based feedback method and two ANC algorithms are

compared through computer simulation in section 3. Cascade ANF, which has a low computational burden, is used to implement the ANC system in real time. The results of the experiments carried out in the laboratory to verify the efficacy of the proposed ANC algorithm are discussed in section 4.

2. FREQUENCY ESTIMATION BASED ON ADAPTIVE NOTCH FILTER

2.1. ADAPTIVE NOTCH FILTER (ANF) WITH CONSTRAINED POLES AND ZEROS

The problem of estimating the frequencies of multiple sinusoids buried in noise has received considerable attention of researchers in the field of signal processing [5–8]. A frequency estimation method that uses ANF with constrained poles and zeros is chosen because of its computational efficiency, fast convergence rate and low threshold SNR [4, 9].

We assume that a signal is composed of multiple sinusoids buried in white noise as follows:

$$x(n) = \sum_{i=1}^{p} U_i \sin(2\pi f_i(n) n + \phi_i) + \xi(n), \tag{1}$$

where $f_i(n)$ is a normalized frequency, which is defined as the frequency divided by the sampling frequency, and $\xi(n)$ is white noise. The transfer function of ANF with constrained poles and zeros is

$$N(z^{-1}) = \frac{A(z^{-1})}{A(\rho z^{-1})} = \frac{1 + a_1 z^{-1} + a_2 z^{-2} + \cdots + a_{2p} z^{-2p}}{1 + \rho a_1 z^{-1} + \rho^2 a_2 z^{-2} + \cdots + \rho^{2p} a_{2p} z^{-2p}}, \tag{2}$$

where ρ, called a pole contraction factor, is a positive real number close to but smaller than 1 and is related to the bandwidth of the notch. Note that the locations of zeros and poles are directly related as follows:

$$P_i = \rho^{-1} Z_i, \quad i = 1, 2, \ldots, p, \tag{3}$$

where P_i is the ith pole and Z_i is the ith zero of $N(z)$.

The ANF has p notches and it can be considered as a prediction error filter with the structure of an autoregressive moving average (ARMA) process. When it turns the signal $x(n)$ into a white signal, which is a desired action of the ANF, the central notch frequencies of the notch filter become the frequencies of the signal $x(n)$ as follows:

$$\hat{f}_i = \frac{1}{2\pi} angle(Z_i | A(z^{-1}) = 0), \quad i = 1, 2, \ldots, p. \tag{4}$$

It is desirable that the zeros of ANF lie on the unit circle. A necessary condition for a polynomial to satisfy this property is that its coefficients will have the mirror symmetric form. Thus, the number of coefficients to estimate is not $4p$ but p, which is due to constraints in poles' and zeros' locations and mirror symmetric property of the numerator of the ANF. We can estimate the coefficients using recursive maximum likelihood method (RML) [4] via the famous stochastic Gauss–Newton

algorithm for an ARMA process. The algorithm has several advantages in the area of accuracy, numerical robustness, stability, convergence speed, computational efficiency and linear phase [4]. However, it is a non-linear recursive least-square (RLS) problem which has local minima due to nonlinearity.

We introduce a frequency estimation algorithm that can offer improved convergence rate, threshold SNR and computational efficiency by linearizing the estimation structure of the notch filter in the following section.

2.2. LINEARIZED MINIMAL PARAMETER ESTIMATION

The linearized minimal parameter estimation algorithm is modified from that of Tranvassor-Romano and Bellanger's [9]. In contrast to their study, a parameter to be estimated is extended to a vector and the mirror symmetric property of the numerator of the ANF is used.

2.2.1 *Basic concept*

The basic concept of the linearized minimal parameter estimation algorithm is to separate the numerator and the denominator of the ANF and update only the numerator as seen in Figure 1. The denominator is obtained from ρ and the numerator $A(z^{-1})$ to be updated in the previous step.

This linearization scheme converts the non-linear RLS problem for an ARMA process into the linear RLS problem for an AR process. Thus, we can expect the problems associated with the nonlinear adaptation to be alleviated. Computational complexity of this algorithm is reduced by $8p + 7$ additions and $21p + 10$ multiplications compared with the RML method. Several advantages of the proposed approach will be presented through simulations in the next section.

2.2.2. *Derivation of the algorithm*

We derive the parameter estimation algorithm for $N(z^{-1})$ in this section:

$$y(n) = \frac{1}{\mathbf{A}(\rho z^{-1})} x(n), \tag{5}$$

$$\boldsymbol{\theta} = [a_1 \cdots a_p]^T. \tag{6}$$

The update equation of the parameter based on the RLS method [10] is

$$\boldsymbol{\theta}(n) = \boldsymbol{\theta}(n-1) + \mathbf{R}^{-1}(n)\boldsymbol{\psi}(n-1)\varepsilon(n), \tag{7}$$

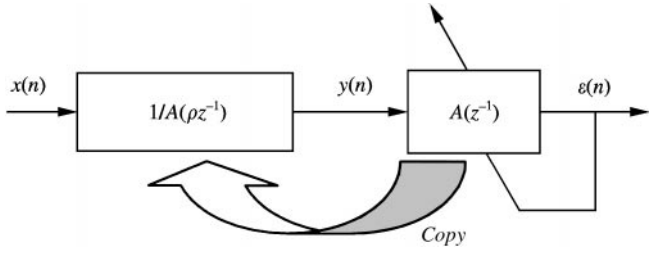

Figure 1. Block diagram of linearized minimal parameter estimation method.

where $\varepsilon(n)$ is a forward prediction error, $\boldsymbol{\psi}(n)$ is a regression vector and $\mathbf{R}(n)$ is a time-varying adaptation gain. They are expressed as

$$\varepsilon(n) = y(n) + y(n-2p) - \boldsymbol{\psi}^T(n-1)\boldsymbol{\theta}(n-1), \tag{8}$$

$$\boldsymbol{\psi}(n-1) = -\frac{\partial \varepsilon(n)}{\partial \boldsymbol{\theta}(n-1)} = [\psi_1(n-1)\cdots\psi_p(n-1)]^T, \tag{9}$$

where

$$\psi_i(n-1) = \begin{cases} -y(n-i) - y(n-2p+i), & 1 \leqslant i \leqslant p-1, \\ -y(n-p), & i = p, \end{cases} \tag{10}$$

$$\mathbf{R}(n) = \sum_{i=1}^{n} \lambda^{n-i}\boldsymbol{\psi}(i-1)\boldsymbol{\psi}(i-1)^T, \tag{11}$$

where λ is a forgetting factor.

Complex computation of the inverse matrix in equation (7) can be avoided by using the matrix inversion lemma [10].

Because the stability of the RLS algorithm can be easily proven without difficulty, it is not included in this paper. The filter $1/A(\rho z^{-1})$ in Figure 1 is stable as well as the filter $\mathbf{A}(z^{-1})$ which is adapted by the RLS algorithm assuming the signal $y(n)$ is bounded.

The linearized minimal parameter estimation algorithm using the ANF with constrained poles and zeros is summarized in Table 1. The q^{-1} is a one-step delay operator.

TABLE 1

Summary of the linearized minimal parameter estimation algorithm

Initialize the algorithm by setting

$\mathbf{P}(0) = \delta^{-1}\mathbf{I}$, δ = a small positive constant, $\boldsymbol{\theta}(0) = 0$, $\boldsymbol{\theta} = [a_1 \cdots a_p]^T$

For each instant of time, $n = 1, 2, \ldots$, compute

$$\mathbf{A}(z^{-1}) = 1 + a_1 z^{-1} + \cdots + a_{p-1}z^{-(p-1)} + a_p z^{-p} + a_{p-1}z^{-(p+1)} + \cdots + a_1 z^{-(2p-1)} + z^{-2p}$$

$$y(n) = \frac{1}{\mathbf{A}(\rho q^{-1})}x(n)$$

$$\boldsymbol{\psi}(n-1) = [\psi_1(n-1)\cdots\psi_p(n-1)]^T, \ \psi_i(n-1) = \begin{cases} y(n-i) + y(n-2p+i), & 1 \leqslant i \leqslant p-1 \\ y(n-p), & i = p \end{cases}$$

$$\mathbf{g}(n) = \frac{\mathbf{p}(n-1)\boldsymbol{\psi}(n-1)}{\lambda + \boldsymbol{\psi}(n-1)^T\mathbf{P}(n-1)\boldsymbol{\psi}(n-1)}$$

$$\varepsilon(n) = y(n) + y(n-2p) + \boldsymbol{\psi}^T(n-1)\boldsymbol{\theta}(n-1)$$

$$\mathbf{P}(n) = \mathbf{P}(n-1)/\lambda - \mathbf{g}(n)\boldsymbol{\psi}(n-1)^T\mathbf{P}(n-1)/\lambda$$

$$\boldsymbol{\theta}(n) = \boldsymbol{\theta}(n-1) - \mathbf{g}(n)\varepsilon(n)$$

2.3. SIMULATION RESULTS

We simulated both the RML method and the proposed one for the multiple sinusoids buried in white noise as noted in equation (1). The input data $x(n)$ were

$$x(n) = 2\sin(2\pi f_1 n) + \sin(2\pi f_2 n) + \xi(n), \tag{12}$$

where the normalized frequencies were 0·15 and 0·17 respectively and $\xi(n)$ was zero-mean white noise. Both algorithms were tested under different SNR conditions. The resulting convergence speeds for four different SNRs are shown in Table 2.

According to Table 2, the proposed algorithm has faster convergence speed than the RML method, while the RML method converges to a local minimum at zero (dB) SNR. We have chosen the optimal convergent step at which the algorithm produces the minimum variance.

The relation between SNR and the variance of frequency estimation error in logarithm scale was seen to be linear in the region with higher SNR than a threshold SNR as illustrated in Figure 2. Threshold SNR is defined as the SNR below which the variance of the estimation error increases drastically.

The y-axis represents the variance of frequency estimation error in logarithmic scale ($\text{err} = f_i - \hat{f}_i$). As shown in Figure 2, the proposed algorithm had a lower threshold SNR than the RML method. This result implies that the proposed algorithm can be applied to noisier system.

Figures 3 and 4 show the tracking capability of the two methods. Dotted and solid lines represent real frequencies and estimated frequencies respectively.

As illustrated in the figures, the proposed algorithm shows better tracking capability than the RML method.

In the simulations, we found good properties of the proposed algorithm such as faster convergence speed and lower threshold SNR than the RML method. We will utilize these beneficial properties in real-time ANC.

3. ANC ALGORITHM BASED ON NOISE FREQUENCY ESTIMATION

3.1. FEEDBACK ANC BASED ON IMC TECHNIQUE

The IMC technique [3] has superior performance over other feedback methods for harmonic noise. The method has a similar structure to the feedforward *filtered-x* LMS algorithm [11] except that a reference signal $r(n+1) = \hat{d}(n)$ is

TABLE 2

Comparison of convergence speed with respect to SNR ($\times$: *local minimum*)

SNR (dB)	200	10	5	0
RML (step)	190	470	510	$\times$
Proposed (step)	110	150	250	450

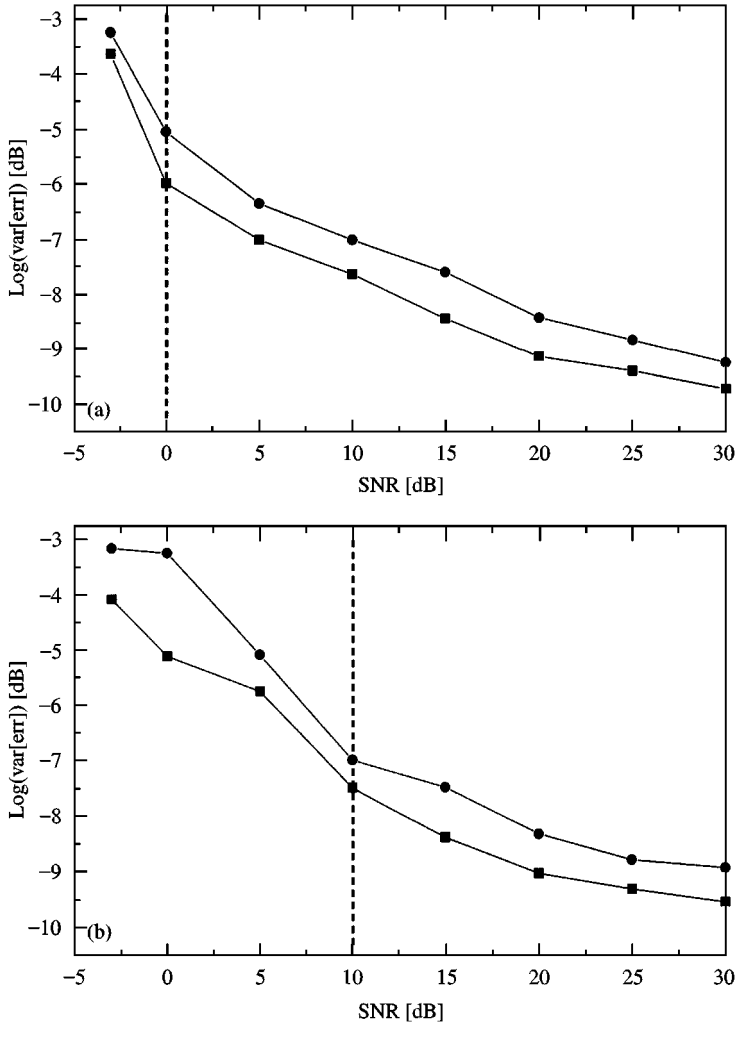

Figure 2. The variance of frequency estimation error with respect to SNR. (a) The proposed algorithm (threshold SNR = 0 dB); (b) the RML method (threshold SNR = 10 dB). —■— f_1; —●— f_2

calculated as

$$\hat{d}(n) = e(n) - \hat{\mathbf{H}} \otimes \mathbf{W} \otimes r(n), \tag{13}$$

where $\mathbf{W}$ is a controller filter, $\hat{\mathbf{H}}$ is a model of the cancellation path, $e(n)$ is a measured error signal and $\otimes$ is a convolution operator. The reference signal $\hat{d}(n)$ is the estimated value of the harmonic noise $d(n)$ generated by the primary noise source, which becomes exact if the model of the cancellation path is perfect. The disturbance $d(n)$ is composed of measurement noise $\xi(n)$ and impulse noise $v(n)$ including a sneeze, clapping of hands and so on as well as sinusoidal components $s(n)$ like

$$d(n) = s(n) + \xi(n) + v(n), \tag{14}$$

where $\xi(n)$ is measurement white noise, $v(n)$ is impulse noise and $s(n)$ is

$$s(n) = \sum_{i=1}^{p} U_i \sin(2\pi f_i(n)n + \phi_i). \tag{15}$$

We can expect good performance when the controller filter is adapted only by the sinusoidal components $s(n)$, which we want to cancel. However, the method is also directly affected by $\xi(n)$ and $v(n)$ as shown in the following rearranged update equation:

$$\mathbf{W}(n+1) = \mathbf{W}(n) - 2\mu e(n)\hat{\mathbf{H}} \otimes r(n) = \mathbf{W}(n) - 2\mu e(n)\hat{\mathbf{H}} \otimes s(n) - 2\mu e(n)\hat{\mathbf{H}} \otimes \{\xi(n) + v(n)\}, \tag{16}$$

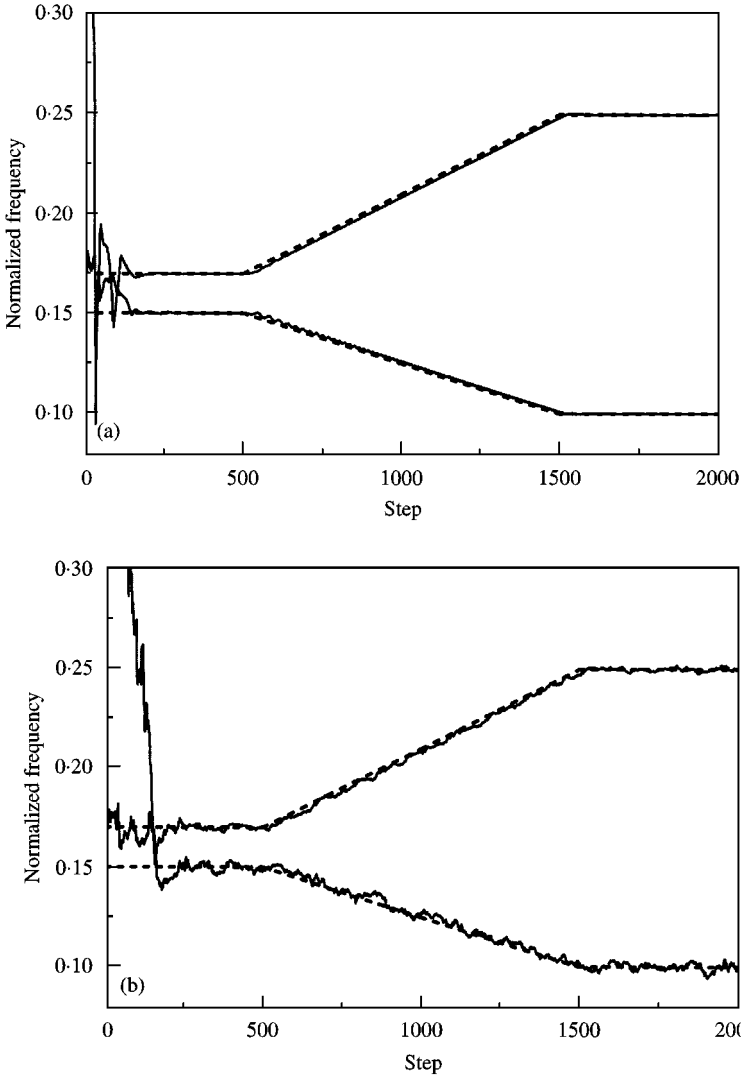

Figure 3. The proposed algorithm (a) SNR = 200 dB; (b) SNR = 0 dB; (c) SNR = 200 dB (crossing). ---- f_1 and f_2; —— estimate of f_1 and f_2.

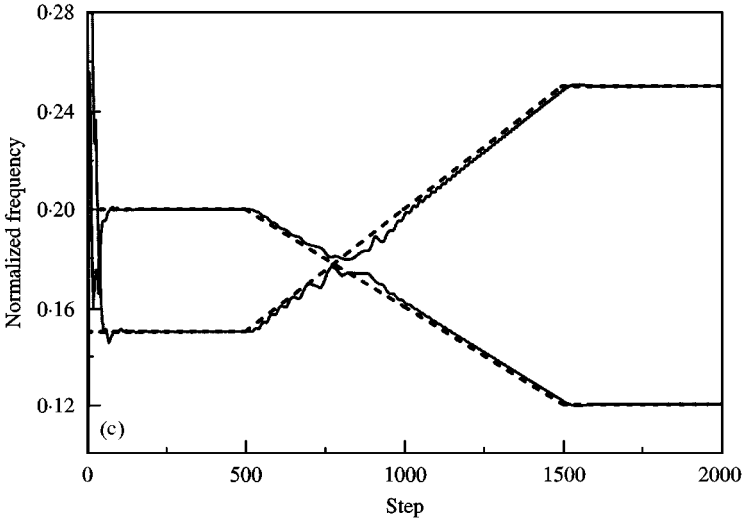

Figure 3. Continued.

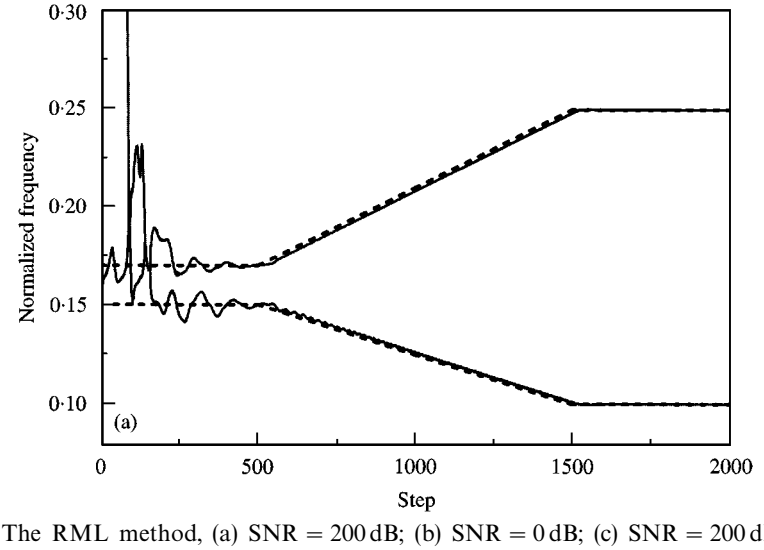

Figure 4. The RML method, (a) SNR = 200 dB; (b) SNR = 0 dB; (c) SNR = 200 dB (crossing). ----f_1 and f_2; —— estimate of f_1 and f_2.

where μ is a step size of filtered-x LMS algorithm. The controller filter can be undesirably excited by the third term of the right-hand side (RHS) of equation (16). In particular, output signals of loud speakers may abruptly increase due to a sudden impulse noise with a large power level, which may drive the ANC system out of control.

3.2. ANC BASED ON NOISE FREQUENCY ESTIMATION

Consider the following three steps for the frequency estimation-based ANC.

Firstly, we estimate the harmonic noise signal cancelled in the controlled field by equation (13). Secondly, we estimate the frequencies of the estimated signal $\hat{d}(n)$ by

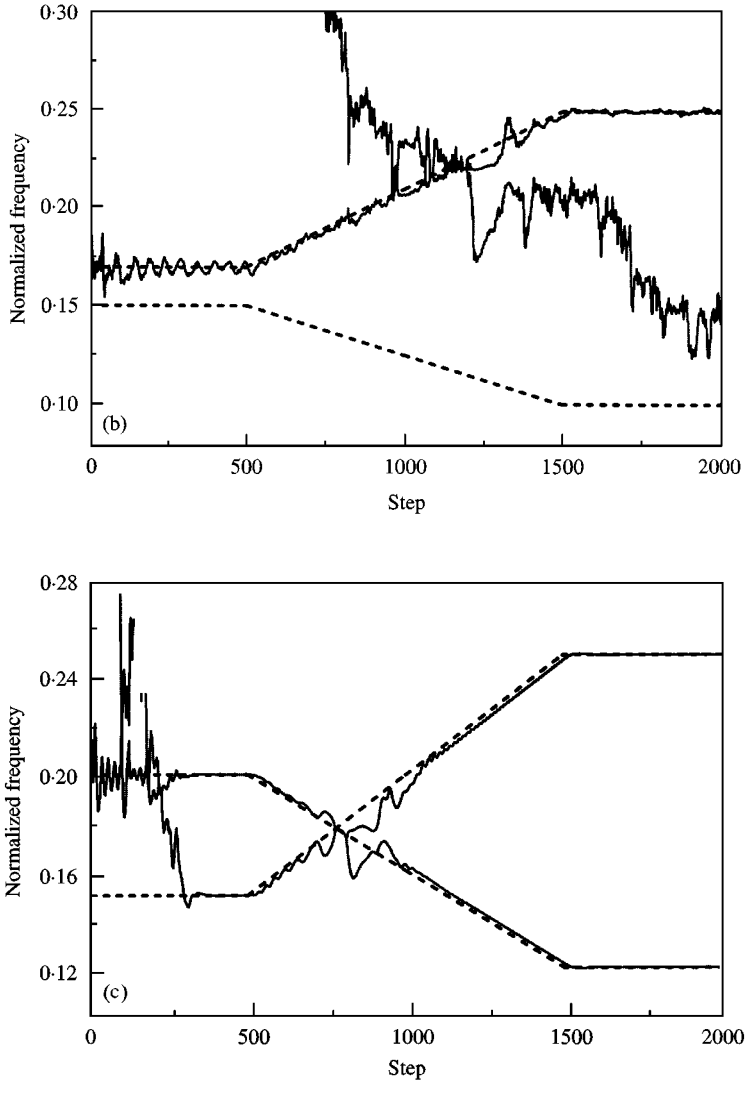

Figure 4. Continued.

the method proposed in section 2. Thirdly, we generate a reference signal as follows:

$$r(n) = \sum_{k=1}^{p} \sin\left(2\pi \sum_{i=0}^{n} \hat{f}_k(n-i)\right), \tag{17}$$

where p is the number of the estimated frequencies and $\hat{f}_k(n-i)$ is the kth estimated frequency of $\hat{d}(n-i)$. It is the kth estimated frequency of $d(n-i)$, if a model of cancellation path is exact and $\hat{d}(n-i)$ is equal to $d(n-i)$. Because impulse noise in equation (14) lasts for a short duration and vanishes, the notch filter would not estimate the frequency of the impulse noise but that of pure harmonic noise $s(n)$. While a reference signal of the method noted in section 3.1 necessarily includes measurement noise or impulse noise, that of the method proposed in this section is

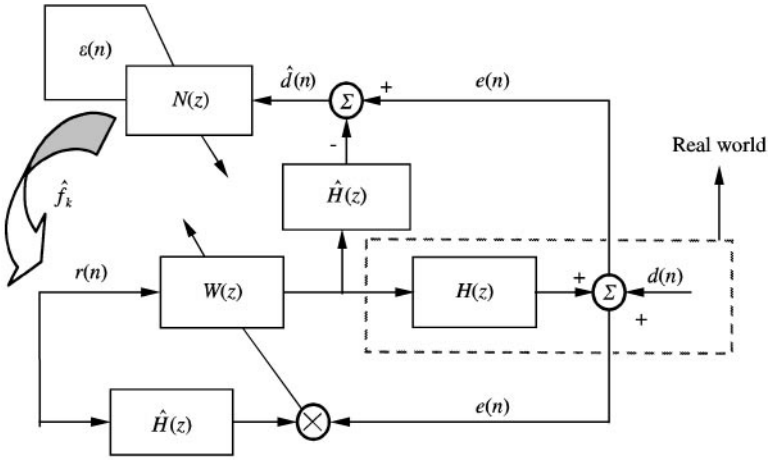

Figure 5. Block diagram of ANC based on noise frequency estimation.

composed of only pure sinusoids as shown in equation (17). Thus, we can expect not only to obtain the performance of a conventional feedforward control, which measures a reference signal correlated with a periodic noise but also to avoid a detrimental effect of measurement noise or impulse noise, assuming accurate estimation of the frequencies. Figure 5 shows the block diagram of the proposed approach. $\mathbf{W}(z)$ is a controller filter, $\mathbf{H}(z)$ is a cancellation path, $\hat{\mathbf{H}}(z)$ is a model of the cancellation path, and the $\mathbf{N}(z)$ is the notch filter mentioned in section 2. $d(n)$ is a disturbance noise and $\hat{d}(n)$ is an estimate of $d(n)$. The lower part of the block diagram is equivalent to a block diagram of the *filtered*-x LMS algorithm [11]. The upper part of the block diagram consists of the part to estimate $d(n)$ and the part to estimate the frequencies of $\hat{d}(n)$.

Moreover, the length of the controller filter does not need to be long for this method while the filter length should be long enough to reduce the effect of measurement noise in the IMC method of section 3.1.

As can be shown in equation (16), the controller filter $\mathbf{W}(z)$ which is adapted by the *filtered*-x LMS algorithm is affected by an error signal $e(n)$ as well as a reference signal $r(n)$ as follows:

$$e(n) = d(n) + \mathbf{H} \otimes \mathbf{W} \otimes r(n) = s(n) + \mathbf{H} \otimes \mathbf{W} \otimes r(n) + \xi(n) + v(n). \tag{18}$$

In order to reduce the effect of the impulse noise or measurement noise included in the error signal, $e(n)$, we define an enhancement error $E(n)$ as

$$E(n) \equiv e(n) - \varepsilon(n), \tag{19}$$

where $e(n)$ is an error signal after ANC and $\varepsilon(n)$ is an output error of the ANF. Assume that the filter $\mathbf{N}(z)$ notches the sinusoidal component $s(n)$. When we adapt the controller filter $\mathbf{W}(z)$ with the enhanced error $E(n)$ instead of the error signal $e(n)$, we can obtain better performance due to the enhanced property of the error

signal as follows:

$$\begin{aligned} E(n) &= e(n) - \mathbf{N}(z)\hat{d}(n) \cong e(n) - \mathbf{N}(z)d(n) \\ &= d(n) + \mathbf{H} \otimes \mathbf{W} \otimes r(n) - \mathbf{N}(z)d(n) \\ &= \mathbf{H} \otimes \mathbf{W} \otimes r(n) + [1 - \mathbf{N}(z)]\{s(n) + \xi(n) + v(n)\}. \end{aligned} \tag{20}$$

From the second term of RHS of equation (20), note that the effect of $\xi(n)$ and $v(n)$ is reduced by a band-pass filter, $[1 - \mathbf{N}(z)]$ which passes only notch frequency component, $s(n)$ of the noise signals.

3.3. SIMULATION RESULTS

We simulated both the IMC method and the proposed ANC for the noise contaminated $d(n)$ in equation (14). Sinusoidal component $s(n)$ of the signal was composed of two tones as in section 2.3. We simulated them for the following two cases to see the effect of the impulse noise and measurement noise respectively.

Case 1: $d(n) = s(n) + v(n)$, where $v(n)$ is impulse noise.

Case 2: $d(n) = s(n) + \xi(n)$, where $\xi(n)$ is additive white noise.

We can see the effect of impulse noise in case 1 and that of measurement noise in case 2. In case 1, we assumed that the exponentially decayed impulse noise occurred after 1000 steps as follows:

$$v(n) = \begin{cases} 0 & \text{for } n < 1000, \\ 10\mathrm{e}^{-0{\cdot}08n} \sin(2\pi\, 0{\cdot}25n) & \text{for } n \geqslant 1000. \end{cases} \tag{21}$$

Note that the controlled error signal includes the incoming impulse noise as well as a controller output signal $y(n)$ affected by it as in equation (22). Therefore, it is hard to see exactly the effect of the impulse noise acting on the controller filter adaptation by plotting the error signal. The controlled error signal with the impulse noise subtracted as in equation (23) can show the effect of the impulse noise acting on the controller filter adaptation more clearly, which is plotted in Figure 6:

$$e(n) = s(n) + v(n) + y(n), \tag{22}$$

$$e(n) - v(n) = s(n) + y(n). \tag{23}$$

In case of the IMC method of section 3.1, the output signal due to the impulse noise suddenly increased because the reference signals included the impulse noise as shown in Figure 6. In case of the proposed algorithm, the output signal was not affected by the impulse noise. Thus, we may say the proposed algorithm is less sensitive to an unexpected impulse noise.

In case 2, $d(n)$ is composed of two tones buried in zero-mean white noise, whose SNR is 10 dB. Figure 7 shows the power spectra of error signals before and after control. Figure 7 illustrates that the proposed algorithm is more efficient than the IMC method in section 3.1.

The controller adaptation of the IMC method was affected by the additive white noise. It led to the increase of the noise in some frequency band as well as the decrease of the amount of the sinusoidal noise reduction. The tonal noise at 150 Hz

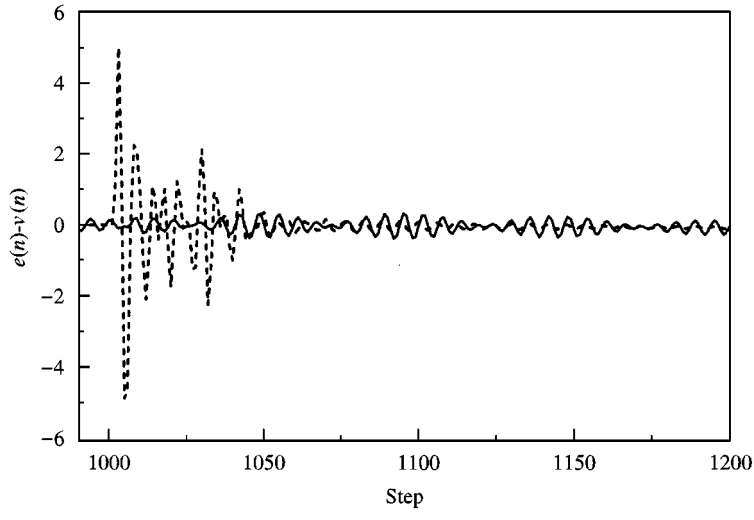

Figure 6. Effect of impulse noise on controller filter. ---- IMC, —— the proposed.

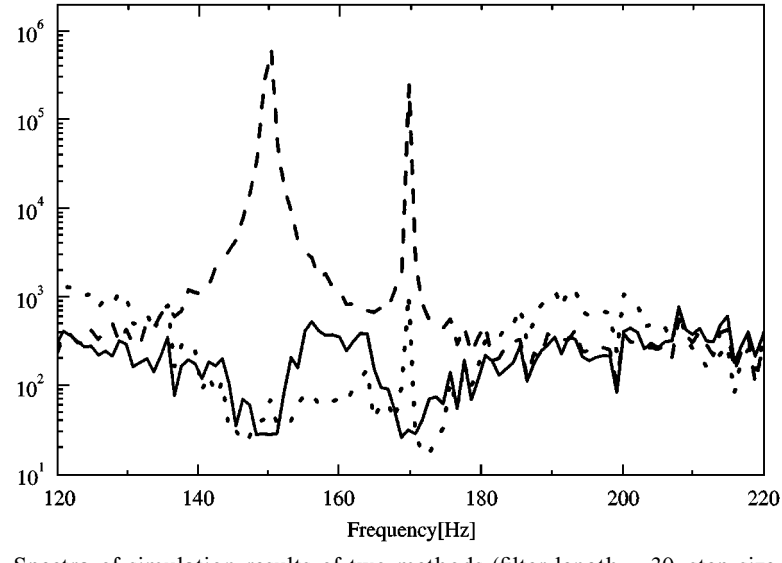

Figure 7. Spectra of simulation results of two methods (filter length = 30, step size = 0·1). – – – before control; . . . . after control (IMC); —— after control (proposed).

was almost cancelled by both the IMC method and the proposed one. The tonal noise at 170 Hz was almost cancelled by the proposed method but was rather weakly cancelled by the IMC method. The same performance can be obtained with the IMC method, if the additive white noise is not added to the sinusoidal noise [12]. In the simulation, we used the sinusoidal noise with the additive white noise as the primary noise. Note that while the IMC method cannot cancel the tonal noise, it can reduce the broadband noise around 160 Hz significantly more than the proposed approach. It is clear that the proposed approach reduced the noise

around the tonal frequencies identified by the adaptive notch filter and does not affect the noise in other frequency range.

To reduce the effect of the measurement noise in the IMC method, the controller filter length should be long. In the proposed algorithm, we can obtain the satisfactory performance with a shorter filter length, if we want to eliminate the tonal components of noise.

4. APPLICATION TO NOISE REDUCTION OF PASSENGER SNIP

4.1. CASCADE ANF FOR LOWER COMPUTATIONAL BURDEN

In real-time control, the computational complexity is a very important issue. To reduce the computational burden in real-time implementations, we use a cascade ANF for the frequency estimation. While a notch filter of order $2p$ is used for p sinusoids in section 3, the cascade ANF is composed of p notch filters of order 2 in series. Each section of the notch filters notches one frequency component of the sinusoids, sequently. Figure 8 shows the block diagram of the cascade ANF.

Note that all the sections of the filter are adapted with error $\varepsilon_p(n)$ of the last section. It is to avoid the conflict in each notch filter. Each section is adapted by the scheme in section 2.2. The algorithm is derived as follows:

$$\varepsilon_k(n) = \mathbf{N}_k(q^{-1})\varepsilon_{k-1}(n). \tag{24}$$

$$\tilde{\varepsilon}_k(n) = \frac{1}{\mathbf{A}_k(\rho q^{-1})}\varepsilon_{k-1}(n) = \varepsilon_{k-1}(n) - \rho a_k(n-1)\tilde{\varepsilon}_k(n-1) - \rho^2\tilde{\varepsilon}_k(n-2), \tag{25}$$

$$\begin{aligned} E_k(n) = {} & \tilde{\varepsilon}_k(n) + \tilde{\varepsilon}_k(n-2) \\ & + \sum_{l=k}^{p-1} \{a_{l+1}(n-1)\varepsilon_l(n-1) + \varepsilon_l(n-2) \\ & - \rho a_{l+1}(n-1)\varepsilon_{l+1}(n-1) - \rho^2\varepsilon_{l+1}(n-2)\}, \end{aligned} \tag{26}$$

$$\Phi_k(n) = \lambda\Phi_k(n-1) + \tilde{\varepsilon}_k(n-1)^2, \tag{27}$$

$$z_k(n) = \lambda z_k(n-1) + \tilde{\varepsilon}_k(n-1)E_k(n), \tag{28}$$

$$a_k(n) = -\Phi_k(n)^{-1} z_k(n), \tag{29}$$

$$f_k(n) = \frac{1}{2\pi}\cos^{-1}\left(-\frac{a_k(n)}{2}\right). \tag{30}$$

Neither a matrix calculation nor a root-finding algorithm is needed and it reduces the computational burden significantly.

We estimated the tonal frequencies of the noisy signal measured in the cabin of a passenger ship to obtain more realistic results. According to the spectrum analysis of the signal, frequency components in the range of 80–180 Hz are dominant. Figure 9 shows the frequency estimation results. Four dominant frequency components are estimated.

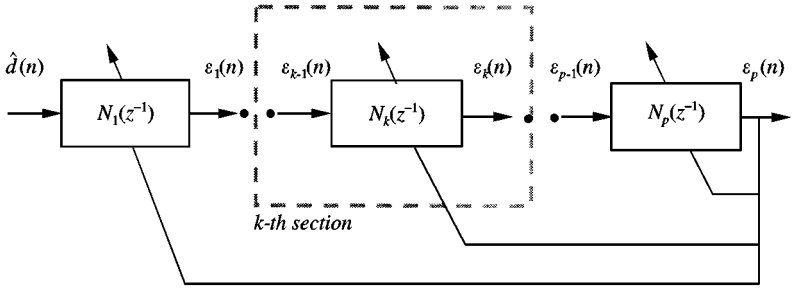

Figure 8. Block diagram of cascade ANF.

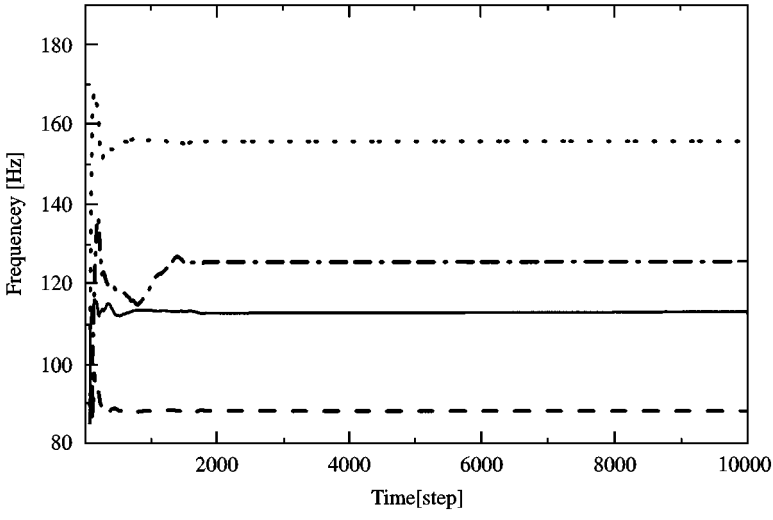

Figure 9. Frequency estimation result. —— f_1; ---- f_2; – – f_3; —·— f_4.

In order to examine the tracking capability of the algorithm, we simulated both the IMC method and the proposed ANC algorithm for two-tone signals with time-varying frequencies. The order of the controller filter is 20, step size is 0·1 and frequency change rate is 10 Hz/s and the sampling frequency is 1 kHz. Figure 10 is a waterfall plot of the error signal before and after control. It illustrates the tracking capability of the proposed ANC algorithm.

As shown in Figure 10, the proposed algorithm has better performance than the IMC method and good tracking capability.

4.2. EXPERIMENTAL RESULTS

The feasibility of the proposed ANC scheme in the application to a passenger ship was verified by experiments in the laboratory where the noise signal measured in the cabin of a passenger ship was generated with a loud speaker.

To obtain a satisfactory performance, two microphones and two speakers were placed near the ears of a person taking a seat as shown in Figure 11.

The schematic diagram of the experimental setup is shown in Figure 12. For the experiments, a TMS320C40 DSP board (*TI Inc.*) connected to a notedbook computer by a local network was used with a 1 kHz sampling frequency. Two

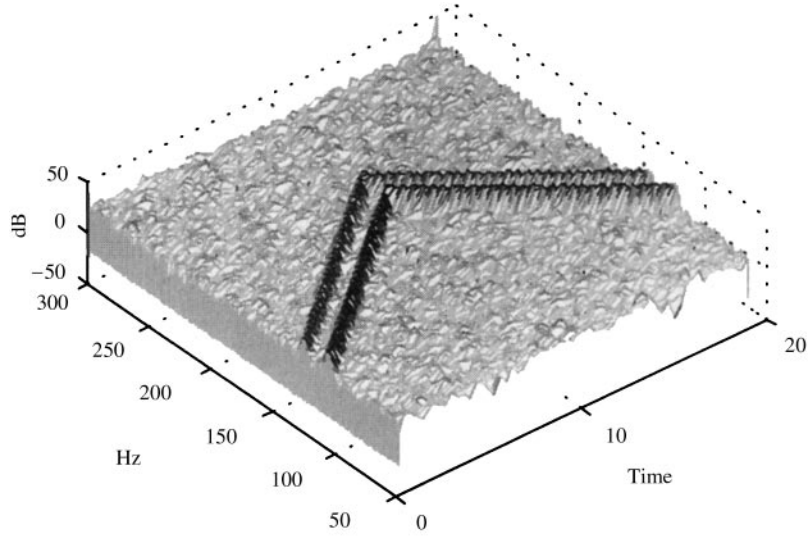

(a)

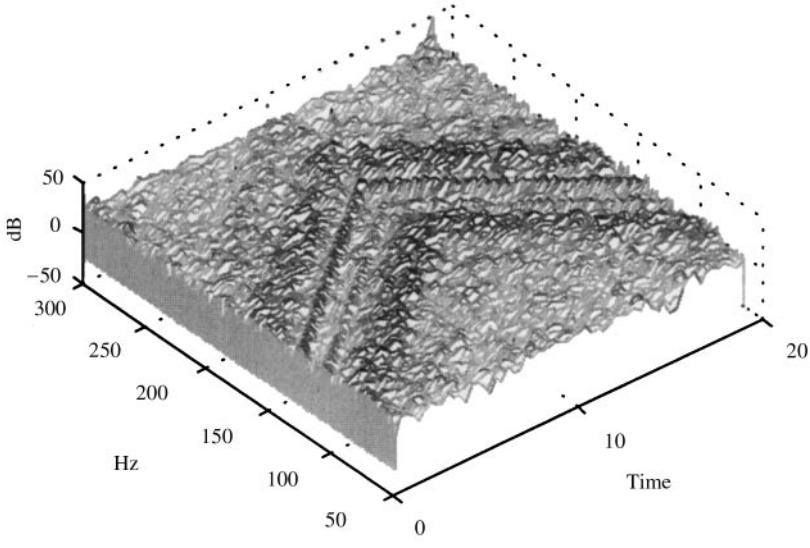

(b)

Figure 10. Waterfall plot of error signals. (a) Error before control; (b) error after control of the IMC method; (c) error after control of the proposed method.

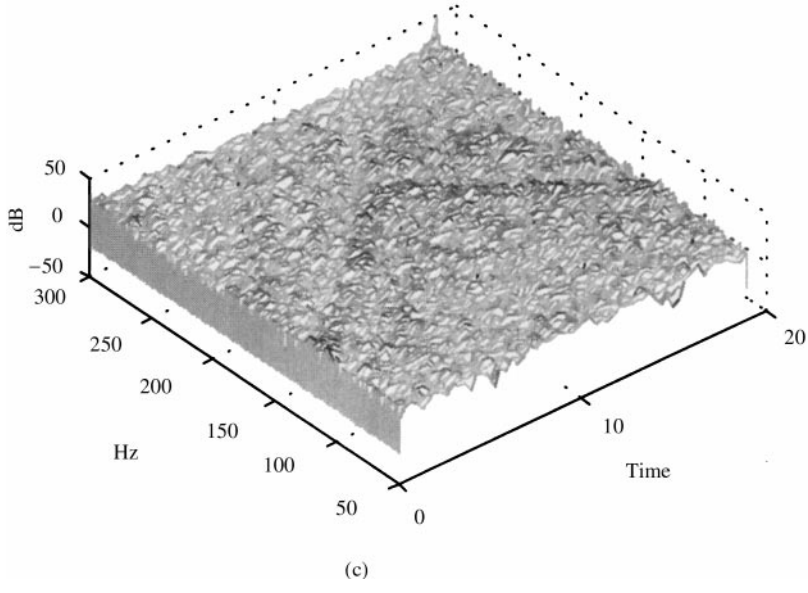

(c)

Figure 10. Continued.

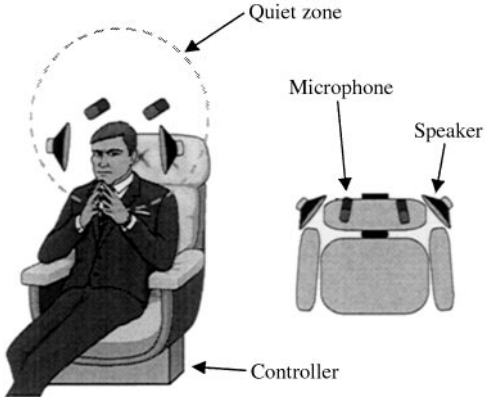

Figure 11. Experimental setup of MIMO ANC system.

low-pass filters with the cut-off frequency of 300 Hz were used as anti-aliasing filters and two low-pass filters with the cut-off frequency of 300 Hz were used for smoothing the D/A output.

Firstly, we estimated the cancellation path with random noise excitation. Secondly, we controlled the engine noise of a passenger ship generated by a loud speaker using the proposed algorithm.

Figure 13 shows the A-weighted steady state power spectra of the error microphone signals before and after real-time control. We used a constrained *filtered*-x LMS algorithm [13] as the feedforward control algorithm.

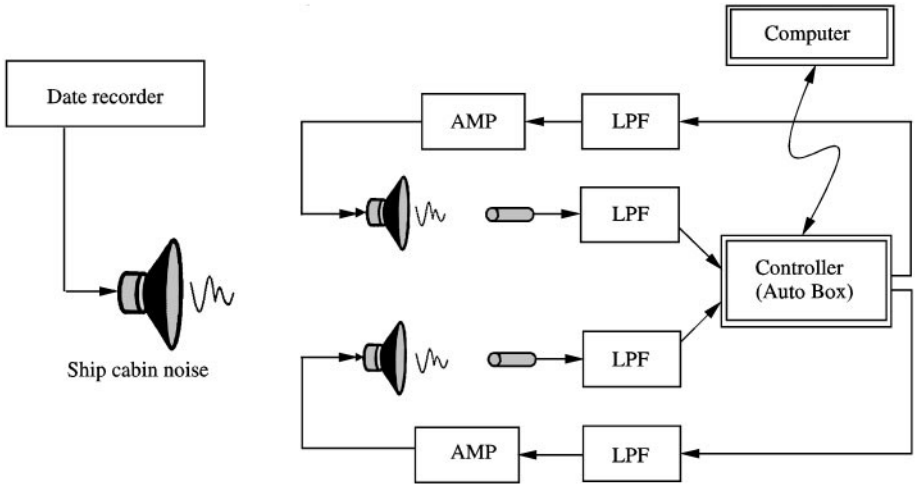

Figure 12. The schematic diagram of the experimental setup.

The notch filter estimated four dominant frequencies exactly and the frequency components were reduced by about 10–20 dB.

5. CONCLUSIONS

We proposed an ANC scheme for harmonic noise reduction, which does not use reference signals. The proposed scheme is composed of two parts. The first part is an on-line frequency estimation. The second part is the conventional feedforward control.

We proposed a new frequency estimation algorithm with an improved convergence rate, threshold SNR and computational efficiency using ANF in real time. We generated the sinusoidal signal with the estimated frequencies, which is used as the reference signal of the feedforward ANC. We compared the proposed algorithm with a feedback method called the IMC technique and obtained superior performance over the conventional approach in terms of sensitivity to measurement noise and impulse noise. We used the cascade ANF for low computational burden in a real-time implementation. We showed the validity of the proposed algorithm for ANC of a passenger ship or multi-tonal noise application through the experiments in the laboratory.

ACKNOWLEDGMENTS

This work was supported by a grant from the Critical Technology 21 Project of the Ministry of Science and Technology, Korea.

The authors would like to thank the HYUNDAI Heavy Industry for providing the ship cabin noise data.

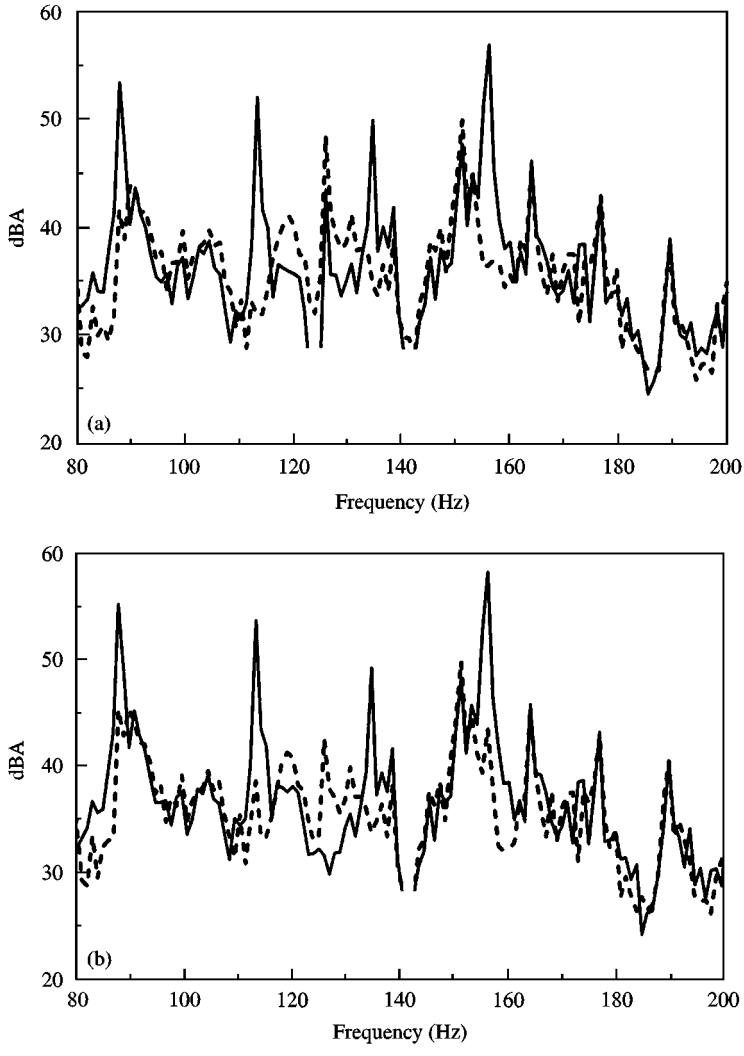

Figure 13. Experimental results of the proposed algorithm (filter length = 70, step size = 0·15). (a) Microphone I; (b) microphone II. —— before control; – – – after control (the proposed)

REFERENCES

1. C. H. Hansen and S. D. Snyder 1997 *Active control of noise and vibration* 374–543. E & FN SPON.
2. S. M. Kuo and D. Vijayan 1994 *Noise Control Engineering* **42**, 37–46. Adaptive algorithms and experimental verification of feedback active noise control systems.
3. S. E. Forsythe, M. D. McCollum and A. D. McCleary 1991 *Proceedings of the Recent Advances in Active Control of Sound and Vibration*, 879–889. Stabilization of a digitally controlled active isolation system.
4. A. Nehorai 1985 IEEE *Transactions on Acoustics, Speech, and Signal Processing*, **33**, 983–996. A minimmal parameter adaptive notch filter with constrained poles and zeros.
5. D. G. Childers 1978 *Modern Spectrum Analysis I*. New York: IEEE Press.
6. S. B. Kesler 1986 *Modern Spectrum Analysis II*. New York: IEEE Press.

7. S. M. Kay and S. L. Marple 1981 *Proceedings IEEE* **69**, 1380–1419. Spectrum analysis—a modern perspective.
8. S. M. Kay 1988 *Modern Special Estimation*: *Theory and Application*. Englewood Cliffs, NJ: Prentice-Hall.
9. J. M. Transvassor-Romano and M. Bellanger 1988 *IEEE Transactions on Acoustics, Speech and Signal Processing* **36**, 1356–1540. Fast least squares adaptive notch filtering.
10. Haykin 1996 *Adaptive Filter Theory*, 3rd pp. 563–588. Englewood Cliff, NJ: Prentice-Hall, third edition.
11. J. C. Burgess 1981 *Journal of Acoustical Society of America* **70**, 715–725. Active adaptive sound control in a duct: a computer simulation.
12. S. J. Elliot and T. J. Sutton 1996 *IEEE Transactions on Speech and Audio Processing* **4**, 214–223. Performance of feedforward and feedback systems for active control.
13. I.-S. Kim, H.-S. Na, K.-J. Kim and Y. Park 1994 *Journal of Acoustical Society of America* **95**, 3376–3389. Constraint filtered-x and filtered-u least mean square algorithms for the active control of noise in ducts.
14. Caplin and Smith, 1986 *US Patent* 4,566,118, Method of and apparatus for cancelling vibrations from a source of repetitive vibrations.